An ENU-Induced Mutation in the *Mertk* Gene (*Mertk*^{nmf12}) Leads to a Slow Form of Retinal Degeneration

Dennis M. Maddox,[1,2] *Wanda L. Hicks,*[1] *Douglas Vollrath,*[3] *Matthew M. LaVail,*[4] *Jürgen K. Naggert,*[1] *and Patsy M. Nishina*[1]

Purpose. To determine the basis and to characterize the phenotype of a chemically induced mutation in a mouse model of retinal degeneration.

Methods. Screening by indirect ophthalmoscopy identified a line of *N*-ethyl-*N*-nitrosourea (ENU) mutagenized mice demonstrating retinal patches. Longitudinal studies of retinal histologic sections showed photoreceptors in the peripheral retina undergoing slow, progressive degeneration. The mutation was named neuroscience mutagenesis facility 12 (*nmf12*), and mapping localized the critical region to Chromosome 2.

Results. Sequencing of *nmf12* DNA revealed a point mutation in the c-mer tyrosine kinase gene, designated *Mertk*^{nmf12}. We detected elevated levels of tumor necrosis factor (*Tnf*, previously *Tnfa*) in retinas of *Mertk*^{nmf12} homozygotes relative to wild-type controls and investigated whether the increase of TNF, an inflammatory cytokine produced by macrophages/monocytes that signals intracellularly to cause necrosis or apoptosis, could underlie the retinal degeneration observed in *Mertk*^{nmf12} homozygotes. *Mertk*^{nmf12} homozygous mice were mated to mice lacking the entire *Tnf* gene and partial coding sequences of the *Lta* (*Tnfb*) and *Ltb* (*Tnfc*) genes.[2] B6.129P2-*Ltb/Tnf/Lta*^{tm1Dvk}/J homozygotes did not exhibit a retinal degeneration phenotype and will, hereafter, be referred to as *Tnfabc*$^{-/-}$ mice. Surprisingly, mice homozygous for both the *Mertk*^{nmf12} and the *Ltb/Tnf/Lta*^{tm1Dvk} allele (*Tnfabc*$^{-/-}$) demonstrated an increase in the rate of retinal degeneration.

Conclusions. These findings illustrate that a mutation in the *Mertk* gene leads to a significantly slower progressive retinal degeneration compared with other alleles of *Mertk*. These results demonstrate that TNF family members play a role in protecting photoreceptors of *Mertk*^{nmf12} homozygotes from cell death. (*Invest Ophthalmol Vis Sci.* 2011;52:4703–4709) DOI:10.1167/iovs.10-7077

Proper function of cells in the retinal pigment epithelium (RPE) is required for normal vision and for the survival of photoreceptor cells. Its importance is underscored by the large number of diseases associated with improper function of the RPE, such as macular edema,[1] Best's vitelliform macular degeneration,[2–4] autosomal recessive macular degeneration,[5] Leber congenital amaurosis,[6–8] and Stargardt disease.[9] Multiple instances of retinitis pigmentosa or allied disorders caused by mutations in the *MERTK* gene have been reported.[10–14] The Royal College of Surgeons (RCS) rat is a classic model for assessing photoreceptor-RPE interaction.[15–17] Mapping efforts determined that a deletion within the *Mertk* gene (*Mertk*^{rdy}) led to a frameshift and a termination signal 20 codons after the start codon in RCS rats.[18,19] Additionally, a targeted mutation of an exon encoding a portion of the *Mer* tyrosine kinase domain in *Mertk*^{tm1Gkm} mice has been reported.[20] This murine allele closely recapitulates the RCS rat phenotype of rapid photoreceptor degeneration.[21] Photoreceptor death in these *Mertk* mutants is associated with an inability of the RPE to properly phagocytize shed photoreceptor outer segment tips.[22,23]

The work presented here is the first to describe a missense mutation in the murine *Mertk* gene (*Mertk*^{nmf12}) associated with retinal degeneration. This mutation exhibits several hallmarks of degeneration reported in other rodent models of *Mertk*-mediated disease; however, the rate of degeneration is much slower in *Mertk*^{nmf12} homozygotes than in RCS rats or *Mertk*^{tm1Gkm} homozygous mice. This slower rate of degeneration offers opportunities to better study the progression of photoreceptor loss under conditions of abnormal MERTK function. Additionally, our studies of the *Mertk*^{nmf12} mutants suggest that TNF family members help to protect homozygous *Mertk*^{nmf12} retinas from degeneration, providing novel insight into mechanisms affecting the rate of photoreceptor degeneration in MERTK-mediated photoreceptor cell death.

Materials and Methods

Mice were bred and housed in standardized conditions in the Research Animal Facility at The Jackson Laboratory and were monitored regularly to maintain a pathogen-free environment. Mice were provided free access to NIH 6% fat chow and acidified water in a vivarium with a 12-hour light/12-hour dark cycle. All mice were treated in accordance with protocols approved by the Animal Care and Use Committee at The Jackson Laboratory, and in compliance with the ARVO Statement for the Use of Animals in Ophthalmic and Vision Research.

Mouse Production and Mapping

A C57BL/6J-*nmf12*/J × DBA/2J F2 intercross was generated by the Speed Expansion IVF (http://jaxmice.jax.org/services /speed expansion.html) service at The Jackson Laboratory. DNA isolated from tail tips of 13 affected and 13 unaffected mice were pooled and subjected to a genome-wide scan using 92 SSLP markers distributed throughout the genome. Samples used in the DNA pools were tested individually to confirm the map location. The critical region was established by genotyping additional recombinant F2 mice with commercially available MIT markers and single

From the [1]Nishina Laboratory and [2]Genetic Resource Sciences, The Jackson Laboratory, Bar Harbor, Maine; [3]Stanford University School of Medicine, Palo Alto, California; and [4]Beckman Vision Center, University of California, San Francisco, California.

Supported by National Eye Institute Grants EY11996 and EY016501 (PMN), EY016313-01 (DMM), a JAX institutional core grant CA34196 (PMN), and the Foundation Fighting Blindness (MML, DV).

Submitted for publication December 16, 2010; revised February 15 and 23 and March 6, 2011; accepted March 7, 2011.

Disclosure: **D.M. Maddox**, None; **W.L. Hicks**, None; **D. Vollrath**, None; **M.M. LaVail**, None; **J.K. Naggert**, None; **P.M. Nishina**, None

Corresponding author: Patsy M. Nishina, The Jackson Laboratory, 600 Main Street, Bar Harbor, ME 04609; patsy.nishina@jax.org.

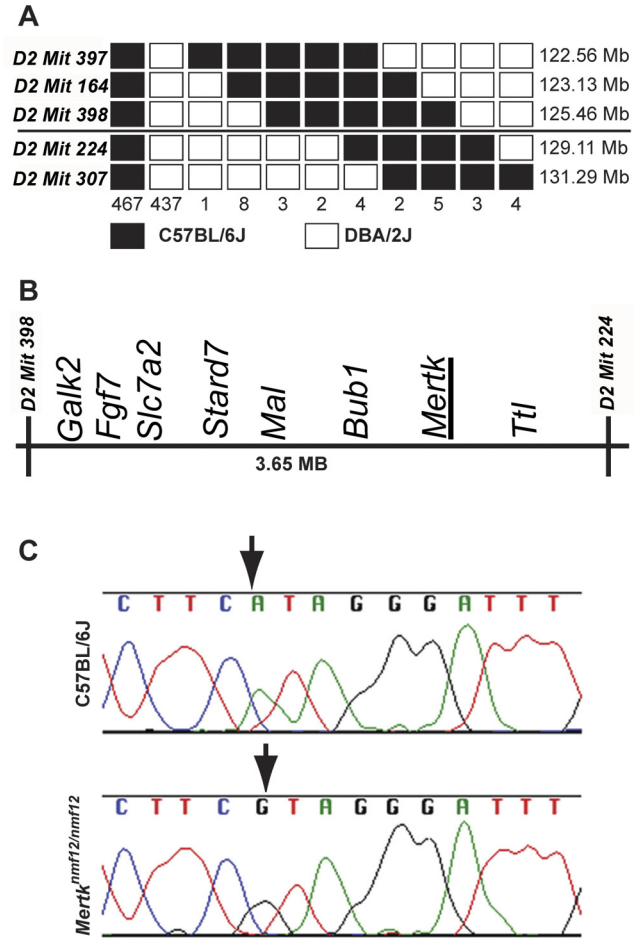

FIGURE 1. Mapping and cloning of the *nmf12* mutation. (**A**) A haplotype map is shown, representing the location and number of crossovers in 936 meioses observed in 468 affected and unaffected progeny-tested mice. The numbers at the bottom of the graph represent the number of chromosomes bearing each depicted crossover. The critical interval spans 3.65 Mb between markers *D2Mit398* (125.46 Mb) and *D2Mit224* (129.11 Mb). Within this critical region (**B**) lies *Mertk*, a gene in which mutations have been shown to cause retinal degeneration. (**C**) Sequence chromatograms from control, C57BL/6J, and *Mertk*^{nmf12} homozygotes. Analysis of these sequences reveals an A-to-G transition at base pair 2237 (A2237G).

nucleotide polymorphisms (SNPs) and was further refined through the generation of additional mapping markers.

Sequencing

Three pairs of eyes isolated from adult *Mertk*^{nmf12} homozygous and wild-type mice were homogenized in a tissue homogenizer (VirTishear; VirTis, Gardiner, NY) for 2 minutes on ice with buffer (Trizol; Invitrogen, Carlsbad, CA). RNA was isolated according to the manufacturer's directions, and the total RNA quality was assessed by running a 5-μL aliquot of each RNA sample on a 1% agarose gel. RNA samples were reverse transcribed into cDNA (RETROscript; Ambion, Austin, TX). The Jackson Laboratory's Allele Typing and Sequencing Facility performed DNA sequencing (Big Dye Terminator chemistry). Data were analyzed with bioinformatics software (MacVector 7.2.3 [MacVector, Inc., Cary, NC] and Sequencher 4.2 [Gene Codes Corporation, Ann Arbor, MI]).

Electroretinography

Full-field ERG recordings were performed as previously described.[24] Briefly, anesthesia was induced by intraperitoneal injection of a mixture of ketamine (70 mg/kg) and xylazine (15 mg/kg), and body temperature (36.5°C-37°C) was maintained with a temperature-controlled heating pad. A gold loop electrode was placed on the surface of the cornea and referenced to a gold wire placed in the mouth. A needle electrode in the tail served as ground. Signals were amplified (×10,000; CP511 AC amplifier; Grass Instruments, Quincy, MA), sampled at 0.8-ms intervals, and averaged. Rod-mediated ERGs were recorded from wild-type and mutant mice that were adapted to darkness overnight and exposed to short-wavelength flashes of light in a Ganzfeld dome (LKC Technologies, Inc., Gaithersburg, MD). Light intensities varied over a 4.0 log unit range up to the maximum allowable by the photopic stimulator (PS33 Plus; Grass Instruments). Cone-mediated responses were obtained with flashes of white light on a rod-saturating background after 10 minutes of light adaptation. Responses were averaged at all intensities, and up to 50 records were averaged for the weakest signals. A signal-rejection protocol was used to eliminate electrical artifacts produced by blinking and eye movements.

Microscopy and Immunohistochemistry

Retinas were fixed in 37.5% methanol/12.5% glacial acetic acid in (1×) phosphate-buffered saline, embedded in paraffin, and sectioned at 6-μm intervals. The sections were subsequently mounted on slides (SuperFrost Plus; Fisher Scientific, Pittsburgh, PA) and were stained with hematoxylin and eosin. Light microscopy and fluorescence microscopy were performed (DMR microscope; Leica, Wetzlar, Germany), and images were collected (FireCam; Leitz). Brightness and contrast of images compared between wild-type and mutant mice were equally optimized (Photoshop 7.0; Adobe, Mountain View, CA). Pri-

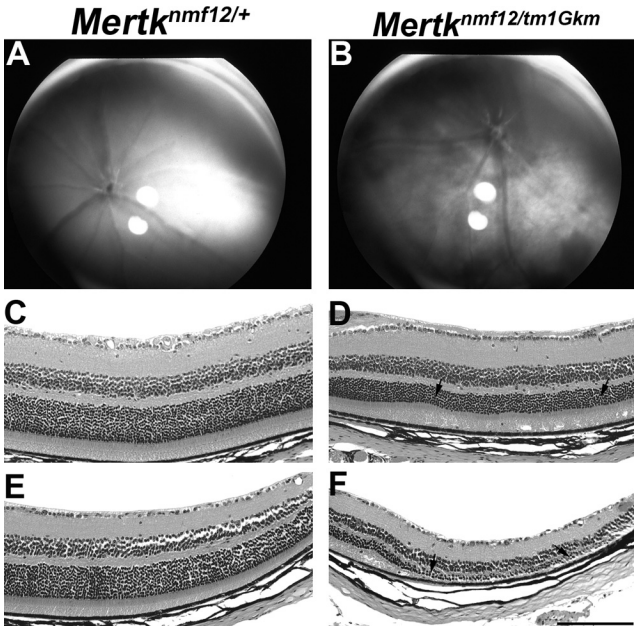

FIGURE 2. Complementation testing between *Mertk*^{nmf12} and *Mertk*^{tm1Gkm}. Indirect ophthalmoscopy shows that at P45, the retinas of *Mertk*^{nmf12}/*Mertk*^{tm1Gkm} compound heterozygous mice demonstrate pan-retinal fundus patches (**B**), whereas the *Mertk*$^{nmf12/+}$ heterozygous littermates (as well as *Mertk*^{nmf12} homozygotes) demonstrate a normal appearance in the central retina (**A**). Histologic examination of central and peripheral sections from the *Mertk*$^{nmf12/+}$ heterozygous littermates (**C** and **E**, respectively) appears normal. In contrast, the central retina of *Mertk*^{nmf12}/^{tm1Gkm} compound heterozygotes (**D**) demonstrates slight thinning of the ONL (*arrows*), whereas the peripheral retina (**F**) demonstrates severe photoreceptor loss (*arrows*). Failure of the *Mertk*^{nmf12}/*Mertk*^{tm1Gkm} compound heterozygous mice to show a normal phenotype provides strong evidence that *Mertk*^{nmf12} and *Mertk*^{tm1Gkm} do not complement and are likely to be allelic mutations. Scale bar, 50 μm (**C**–**F**).

mary antibodies were used at the concentration of 1:200. Appropriate secondary antibodies conjugated to either CY3 (Jackson Immunochemicals, West Grove, PA) or Alexa-488 (Molecular Probes, Eugene, OR) were applied at a dilution of 1:500.

Western Blot Analysis

Six eyes each from C57BL/6J and C57BL/6J-*Mertk*^{nmf12}/J homozygous mice were homogenized in 300 μL RadioImmuno Precipitation Assay (RIPA) buffer containing protease inhibitor cocktail (Roche Diagnostics, Indianapolis, IN). Protein concentrations were determined using the Bio-Rad Protein Assay (Bio-Rad Laboratories, Inc., Hercules, CA), and 40 μg total protein for each sample was loaded with sample buffer (NuPAGE LDS; Invitrogen) and sample reducing agent (NuPAGE; Invitrogen). Samples were run on a 10% Bis-Tris gel with MOPS/SDS running buffer (NuPAGE; Invitrogen). Samples were transferred overnight onto a polyvinylidene difluoride (PVDF) membrane (Roche Diagnostics), and the membrane was blocked for 1 hour in Tris-buffered saline plus 5% milk powder before being probed with a polyclonal antibody against MERTK (af591) (R&D Systems, Minneapolis, MN). After washing, the membrane was probed with peroxidase-conjugated donkey anti-rabbit IgG (1:40,000; AffiniPure; Jackson ImmunoResearch, Inc.), and signal was detected with Western Lightning Chemiluminescent Reagent (Perkin Elmer Life Sciences, Inc., Waltham, MA).

Results

Mapping and Identification of the *Mertk*^{nmf12} Mutation

By in vitro fertilization, we generated a C57BL/6J-*nmf12/nmf12* X DBA/2J F1 intercross, simultaneously producing 468 mice (representing 936 meioses) for mapping. A total of 32 F2 mice were identified with genetic crossovers between flanking markers *D2Mit397* (122.56 Mb) and *D2Mit307* (130.10 Mb). These 32 crossover mice were genotyped with a combination of MIT markers and SNPs (Fig. 1A), and the critical region was reduced to a 3.65-Mb region between markers *D2Mit398* (125.46 Mb) and *D2Mit224* (129.11 Mb; Fig. 1B). Within this critical region were 56 annotated transcripts, one of which encodes the *Mertk* gene. Sequencing of *Mertk* cDNA from *Mertk*^{nmf12} homozygotes revealed a G-to-A substitution at base pair 2237 (Ensembl build 42: OTTMUSP0000016359; Fig. 1C). As further confirmation that the mutation in *Mertk* was causative of the observed retinal degenerative phenotype in *Mertk*^{nmf12} homozygotes, we performed a complementation test between homozygous *Mertk*^{nmf12} mice and mice carrying a targeted deletion (*Mertk*^{tm1Gkm}) in the *Mertk* gene.[20] *Mertk*^{nmf12} is not capable of complementing *Mertk*^{tm1Gkm} (Fig. 2), offering strong evidence that the two mutations are allelic.

Analysis of *Mertk*^{nmf12} Protein Expression

The missense mutation found in *Mertk*^{nmf12} mutants causes a substitution at amino acid position 716 (Fig. 3A) and is predicted to alter a highly conserved histidine residue to arginine (H716R; Fig. 3B). This residue is located within the tyrosine kinase domain of the MERTK protein (Fig. 3C). Immunohistochemical studies showed that MERTK protein was present and properly localized to the RPE of *Mertk*^{nmf12} homozygotes (data not shown). To determine whether this mutation could destabilize the MERTK protein and lead to its early degradation, Western blot analysis was performed. A 2.5-fold reduction in MERTK protein was evident in retinas of *Mertk*^{nmf12} homozygotes (Fig. 3D).

Analysis of *Mertk*^{nmf12} Retinal Phenotype

Mertk^{nmf12} mutants were first identified by screening ENU-mutagenized mice by indirect ophthalmoscopy. The peripheral retina of *Mertk*^{nmf12} homozygotes, when viewed by indirect ophthalmoscopy, appeared depigmented as early as postnatal day (P) 30 (data not shown). As the *Mertk*^{nmf12} homozygotes age, patches become evident in the central portion of the

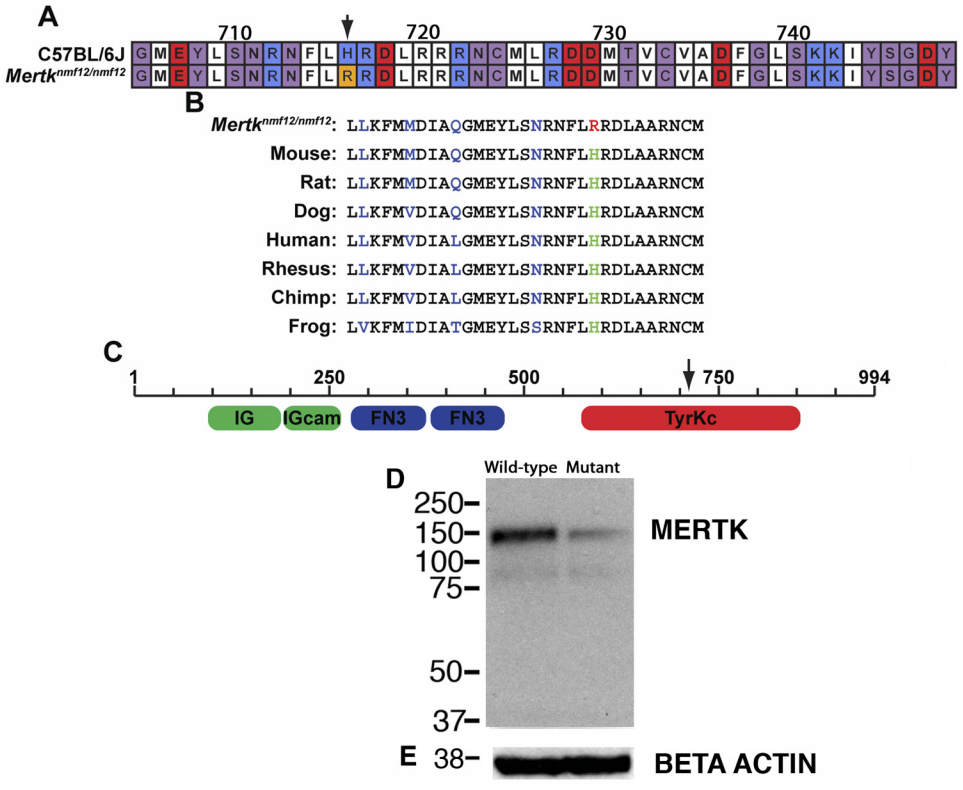

Figure 3. Analysis of *Mertk*^{nmf12} protein expression and function. (**A**) Depiction of protein alignment between C57BL/6J and *Mertk*^{nmf12} homozygotes (amino acids presented in randomly selected colors). A substitution of arginine for histidine is evident at amino acid 716 (H716R; *arrow*). This residue is conserved across species (**B**). (**C**) Schematic showing that the mutated amino acid falls within the tyrosine kinase domain of the *Mertk* gene. Western blot analysis shows a 2.5-fold reduction of MERTK protein in *Mertk*^{nmf12} homozygous retinas (**D**). The blot was stripped and probed again with an antibody against β-actin as a loading control (**E**).

retina in addition to those observed in the periphery (Figs. 4A, 4B). When viewed by histology at P30, wild-type mice have normal, well-structured retinas (Fig. 4C). *Mertk*^{nmf12} homozygous retinas, when viewed at P30, demonstrate thinning of the peripheral outer nuclear layer (ONL; Fig. 4D). As time progresses, photoreceptor cell death increases and the ONL becomes increasingly thinner (Fig. 4E). As the majority of photoreceptors die, a single layer of photoreceptor nuclei is left adjacent to the RPE in the peripheral retina (Fig. 4F). Although the death of photoreceptor nuclei is most dramatic in the peripheral retina, presence of apoptotic nuclei is evident throughout the mutant retina at P45 (Figs. 4G, 4H). Most photoreceptors in the central retina, however, are spared (data not shown), and though electroretinographic (ERG) recordings do become progressively attenuated, ERG a- and b-waves are detectable in *Mertk*^{nmf12} homozygotes as old as 2 years of age (Fig. 5).

Analysis of TNF Expression in *Mertk*^{nmf12} Eyes

Studies involving *Mertk*^{tm1Gkm} homozygotes have demonstrated that serum levels of TNF are increased because of an inability of macrophages to phagocytize apoptotic nuclei.[20,25] The increased TNF levels are thought to cause cellular damage and lethal tissue injury, and the small intestines of *Mertk*^{tm1Gkm} homozygotes were shown to be damaged as a result of excess TNF. Therefore we investigated whether TNF levels were increased in retinas of *Mertk*^{nmf12} homozygotes. Immunohistochemistry with an antibody directed against TNF (ab9739; Abcam) was performed on wild-type (Figs. 6A, 6C) and *Mertk*^{nmf12} homozygous (Figs. 6B, 6D) retinas. A marked increase in staining was observed in retinal sections from the *Mertk*^{nmf12} homozygotes compared with controls.

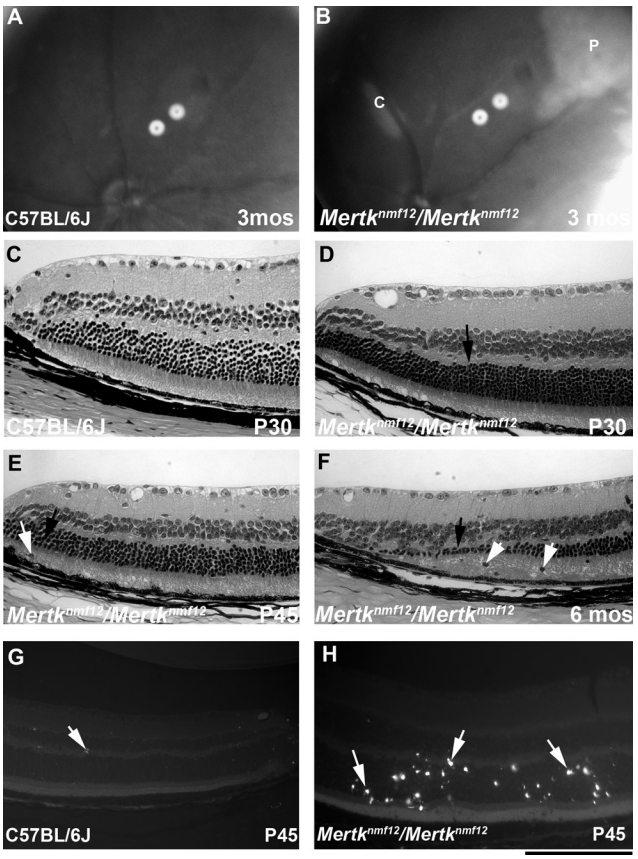

FIGURE 4. Analysis of the *Mertk*^{nmf12} retinal phenotype. Fundus photographs of 3-month-old C57BL/6J (**A**) or homozygous *Mertk*^{nmf12} (**B**) mice. Note the abnormal whitening of the peripheral (P) and central (C) retina that is likely to correspond to areas of ONL degeneration. Histologic sections of the peripheral retina from a P30 C57BL/6J mouse (**C**). The ONL in retinas of *Mertk*^{nmf12} homozygotes aged P30, P45, and 6 months are shown (**D**–**F**, respectively). (**D**, *arrow*) Beginning of ONL cell thinning. This ONL thinning progresses over time. (**E**, **F**, *black arrows*) Thinning ONL. Pyknotic nuclei are present (**E**, **F**, *white arrows*) suggesting that cell death is taking place. Few TUNEL-positive cells (*white arrow*) are present in the retinas of P45 C57BL/6J mice (**G**), whereas many TUNEL-positive cells (*white arrows*) are present throughout the ONL in retinas of *Mertk*^{nmf12} homozygotes (**H**). Scale bar, 50 μm (**C**–**H**).

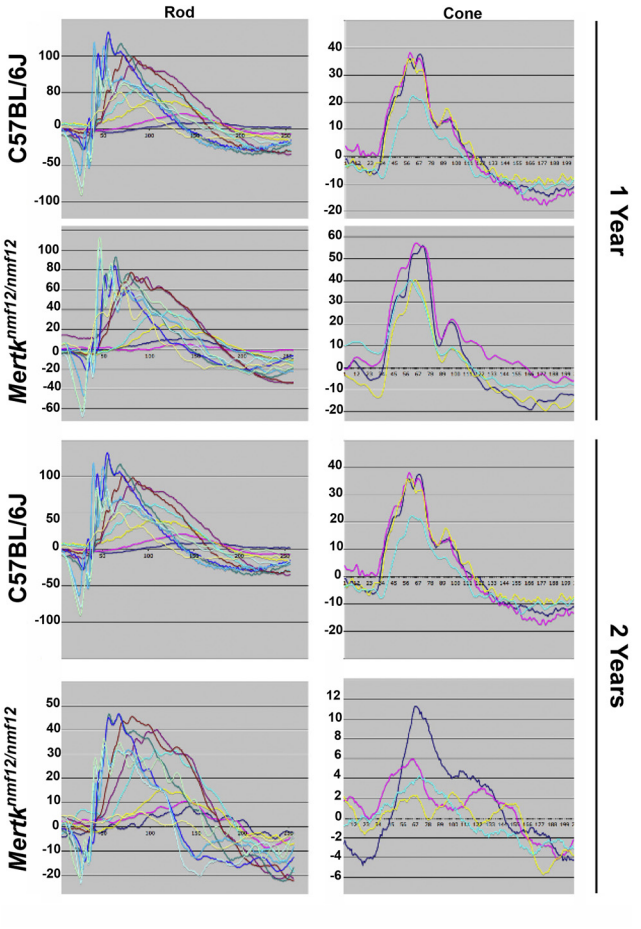

FIGURE 5. Analysis of the ERG function in eyes of *Mertk*^{nmf12} mutants. Although dying cells are present throughout the retinas of *Mertk*^{nmf12} homozygotes, the majority of photoreceptor cells in the central portion of the retina of *Mertk*^{nmf12} homozygotes are preserved. This preservation is reflected in the ERG waveforms. Although the amplitude of the waveforms recorded from homozygous *Mertk*^{nmf12} retina are progressively reduced over time compared with those of C57BL/6J mice, ERG waveforms are still detectable from eyes of *Mertk*^{nmf12} homozygotes aged up to 2 years.

Genetic Manipulation of Tumor Necrosis Factor Levels in *Mertk*^{nmf12} Mutant Eyes

To ascertain the effect of increased TNF levels in the retinas of *Mertk*^{nmf12} homozygotes, we performed a genetic experiment in which *Mertk*^{nmf12} homozygotes were crossed to *Tnfabc*$^{-/-}$ homozygotes, and the resultant F1 offspring were intercrossed. *Mertk*^{nmf12}*/Mertk*^{nmf12}*; Tnfabc*$^{-/-}$ double homozygous mice exhibited an increased rate of photoreceptor cell degeneration compared with littermate mice homozygous for the *Mertk*^{nmf12} mutation alone. At P45, when examined by indirect ophthal-

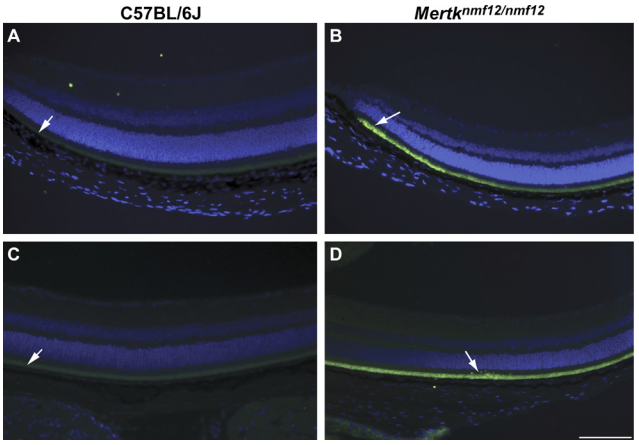

FIGURE 6. Immunohistochemical analysis of TNF expression in eyes of *Mertk*^{nmf12} mutants. TNF is faintly present in the outer retina in peripheral (**A**) and central (**C**) retinas of C57BL/6J mice (*white arrows*). In comparison, TNF fluorescence is much more intense in the outer retina in the peripheral (**B**) and central (**D**) regions of *Mertk*^{nmf12} homozygous retinas (*white arrows*). Scale bar, 50 μm (**A–D**).

moscopy, the central retinas of *Mertk*^{nmf12}/*Mertk*^{nmf12}; *Tnfabc*$^{-/-}$ double homozygotes (Fig. 7B) demonstrated an abnormal appearance across the entire retina, whereas the central retinas of homozygous *Mertk*^{nmf12} mice appeared normal (Fig. 7A). Histologically, at 1 month of age, the thicknesses of *Mertk*^{nmf12} homozygous ONL in the central (Fig 7C) and peripheral (Fig 7D) retina were similar to those observed for *Mertk*^{nmf12}/*Mertk*^{nmf12}; *Tnfabc*$^{-/-}$ mice (Figs. 7E, 7F). At 3 months of age, the central retina of *Mertk*^{nmf12} homozygotes appeared relatively normal (Fig. 7G), whereas slight thinning of the ONL was evident in the peripheral retina (Fig. 7H). Demonstrating an accelerated rate of degeneration, the ONL of *Mertk*^{nmf12}/*Mertk*^{nmf12}; *Tnfabc*$^{-/-}$ double mutant mice was markedly thinned pan-retinally at 3 months of age (Figs. 7I, 7J), with an additional loss of cells in the inner nuclear layer in the peripheral retina.

DISCUSSION

We have demonstrated that the *nmf12* mutation maps to Chromosome 2 and that the observed phenotype segregates with a point mutation in the *Mertk* gene. This mutation leads to the replacement of a conserved histidine residue, within the MERTK tyrosine kinase domain, with arginine. The failure to complement the *Mertk*^{tm1Gkm} allele and the reduced levels of MERTK protein in *Mertk*^{nmf12} homozygotes provide strong evidence that the missense mutation detected in the *Mertk* gene causes the observed retinal phenotype.

The ONL of *Mertk*^{tm1Gkm} homozygotes is almost completely normal at P20.[21] Soon afterward (P25), the ONL becomes significantly thinned throughout the entire retina. Most photoreceptor nuclei are missing by P45, and no ERG activity is readily discernible after P40.[21] In contrast, retinal thinning proceeds slowly from the periphery toward the central retina in *Mertk*^{nmf12} homozygotes, and normal ONL thickness is preserved in the central retina of *Mertk*^{nmf12} homozygotes as old as 2 years of age. Because of this conservation of the central retina, ERG measurements are also recordable up to 2 years of age in *Mertk*^{nmf12} homozygotes.

The *Mertk*^{tm1Gkm} allele was generated by targeting an exon that encodes essential portions of the tyrosine kinase domain of MERTK.[20] Whether the difference in the rate of retinal degeneration was due to allelic variance or genetic background is uncertain because the *nmf12* allele arose on a mutagenized C57BL/6J background, whereas the *Mertk*^{tm1Gkm} mutant allele was targeted in a 129/Sv background and was maintained on a mixed genetic background of C57BL/6J and 129/Sv. It is interesting to note as well that the *Mertk*^{tm1Gkm} allele was not intended to be a null allele.[20] Given that the rate of retinal degeneration in *Mertk*^{tm1Gkm} mutant mice is rapid and comparable to that seen in the rat *Mertk*^{rdy} null allele and that no truncated protein is detectable in kidney or retina samples from *Mertk*^{tm1Gkm} mutant mice, the *Mertk*^{tm1Gkm} allele does

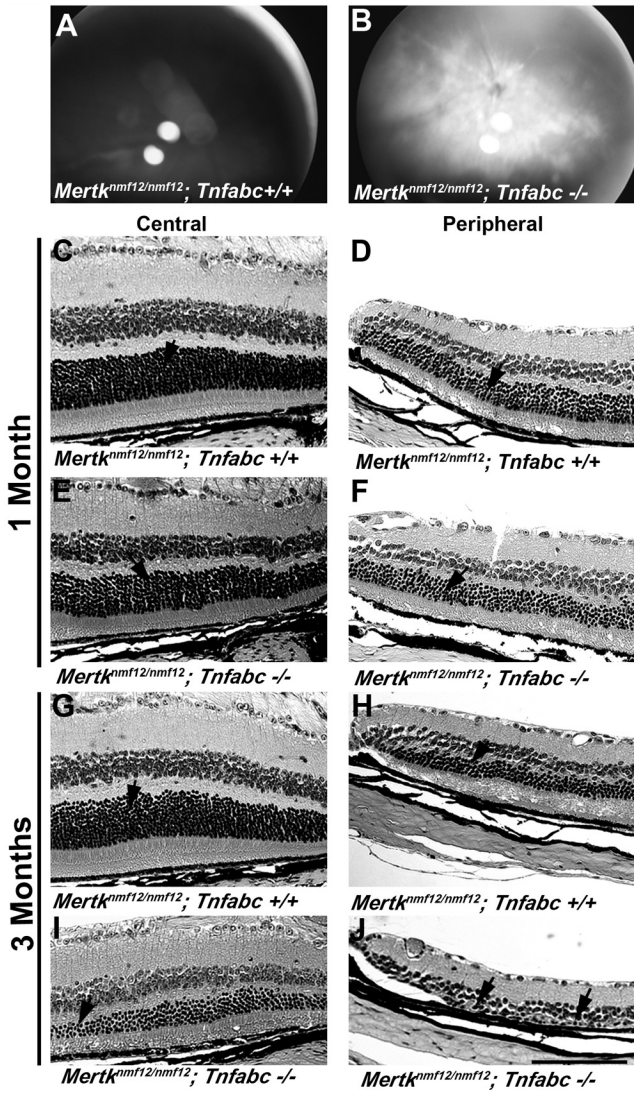

FIGURE 7. Genetic manipulation of tumor necrosis factor levels in eyes of *Mertk*^{nmf12} mutants. Fundus photographs of P45 *Mertk*^{nmf12}/*Mertk*^{nmf12}; *Tnfabc*$^{+/+}$ (**A**) and *Mertk*^{nmf12}/*Mertk*^{nmf12}; *Tnfabc*$^{-/-}$ (**B**) mice are presented. Note the pan-retinal patches in the latter. Histologic sections are of central (**C**) and peripheral (**D**) retinas of a 1-month-old *Mertk*^{nmf12}/*Mertk*^{nmf12}; *Tnfabc*$^{+/+}$ retina and central (**E**) and peripheral (**F**) retinas of an age-matched *Mertk*^{nmf12}/*Mertk*^{nmf12}; *Tnfabc*$^{-/-}$ mouse. The thickness of the ONL is similar between *Mertk*^{nmf12}/*Mertk*^{nmf12}; *Tnfabc*$^{+/+}$ and *Mertk*^{nmf12}/*Mertk*^{nmf12}; *Tnfabc*$^{-/-}$ mice (*arrows*). Central (**G**) and peripheral (**H**) retinas of a 3-month-old *Mertk*^{nmf12}/*Mertk*^{nmf12}; *Tnfabc*$^{+/+}$ retina and central (**I**) and peripheral (**J**) retinas of an age-matched *Mertk*^{nmf12}/*Mertk*^{nmf12}; *Tnfabc*$^{-/-}$ retina are presented. Although the ONL of *Mertk*^{nmf12}/*Mertk*^{nmf12}; *Tnfabc*$^{+/+}$ retinas remains relatively intact (**G**, **H**, *arrows*), extensive thinning of the ONL is evident in the central and peripheral retina (**I**, **J**, arrows, respectively) of the *Mertk*^{nmf12}/*Mertk*^{nmf12}; *Tnfabc*$^{-/-}$ mice. Scale bar, 50 μm (**C–J**).

appear to be null.[21] The *Mertk*^{nmf12} allele also affects the tyrosine kinase domain of MERTK but is a point mutation. In contrast to what is seen in the *Mertk*^{tm1Gkm} mutant mice, MERTK protein is detectable in retinal samples of *Mertk*^{nmf12} mutant mice, though at a reduced amount compared with wild-type controls. Thus, the *Mertk*^{nmf12} mutant protein may retain some functional activity and thereby cause a slower rate of photoreceptor cell loss than that observed in previously described models.

After the work of Camenisch et al.,[20] who reported increased serum TNF levels in *Mertk*^{tm1Gkm} and associated this accumulation with tissue damage in the small intestine, we undertook to determine whether TNF levels were increased in the retinas of *Mertk*^{nmf12} homozygous mice. Our immunohistochemical studies suggest that TNF levels are increased in the retinas of *Mertk*^{nmf12} homozygous mice compared with those of wild-type controls. TNF is a cytokine that produces paradoxical effects in various instances. The role of TNF in uveoretinitis has been studied in depth, with increased TNF levels most often preceding tissue damage.[26] Similarly, in many other types of retinal disease, increased levels of TNF are associated with increased retinal degeneration. Because of this, TNF inhibitory antibodies (infliximab, etanercept) have been developed and are being used in trials to treat human diseases such as age-related macular degeneration,[27] Eales disease,[28] neurosarcoidosis,[29] various forms of ocular inflammation,[30] diffuse subretinal fibrosis syndrome,[31] and glaucoma.[32]

As has been noted[33] and as our present study underscores, there are instances in which TNF plays a poorly understood protective role in retinal degeneration. It has been posited that in retinas of *Mertk*^{rdy} rats, the RPE secretes a factor that might attract phagocytic cells, such as microglia, to help restore an environment more conducive to photoreceptor survival.[34] Our studies suggest that TNF may be this predicted factor. That the loss of TNF function could potentially lead to deleterious effects should certainly be kept in mind when administering TNF inhibitors to human patients, and *Mertk*^{nmf12} mutant mice offer a powerful tool to better illuminate the protective role TNF can play in various forms of retinal degeneration.

Acknowledgments

The authors thank Jeanie Hansen for excellent technical assistance and The Jackson Laboratory's Fine Mapping Service for performing the initial steps in the mapping process.

References

1. Marmor MF. Mechanisms of fluid accumulation in retinal edema. *Doc Ophthalmol.* 1993;97:179–203.
2. Allikmets R, Seddon JM, Bernstein PS, et al. Evaluation of the Best disease gene in patients with age-related macular degeneration and other maculopathies. *Hum Genet.* 1999;104:449–453.
3. Bakall B, Marknell T, Ingvast S, et al. The mutation spectrum of the bestrophin protein- functional implications. *Hum Genet.* 1999; 104:338–389.
4. Caldwell GM, Kakuk LE, Griesinger IB, et al. Bestrophin gene mutations in patients with Best vitelliform macular dystrophy. *Genomics.* 1999;58:98–101.
5. Ambati J, Ambati BK, Yoo SH, Ianchulev S, Adamis AP. Age-related macular degeneration: etiology, pathogenesis and and therapeutic strategies. *Surv Ophthalmol.* 2003;48:257–293.
6. Hamel CP, Tsilou E, Pfeffer BA, Hooks JJ, Detrick B, Redmond TM. Molecular cloning and expression of RPE65, a novel retinal pigment epithelium-specific microsomal protein that is post-transcriptionally regulated in vitro. *J Biol Chem.* 1993;268: 15751–15757.
7. Hamel CP, Jenkins NA, Gilbert DJ, Copeland NG, Redmond TM. The gene for the retinal pigment epithelium-specific protein, RPE65, is localized to human 1p31 and mouse 3. *Genomics.* 1994; 20:509–512.
8. Hamel CP, Griffion JM, Lasquellec L, Bazalgette C, Arnaud B. Retinal dystrophies caused by mutations in RPE65: assessments of visual functions. *Br J Ophthalmol.* 2001;85:424–427.
9. Simonelli F, Testa F, de Creechio G, et al. New ABCR mutations and clinical phenotype in Italian patients with Stargardt disease. *Invest Ophthalmol Vis Sci.* 2000;41:892–897.
10. Gal A, Li Y, Thompson DA, et al. Mutation in MERTK, the human orthologue of the RCS rat retinal dystrophy gene, cause retinitis pigmentosa. *Nature.* 2000;26:270–271.
11. Thompson DA, McHenry CL, Li Y, et al. Retinal dystrophy due to paternal isodiomy for chromosome 1 or chromosome 2, with homoallelism for mutations in RPE65 or MERTK, respectively. *Am J Hum Genet.* 2002;70:224–229.
12. McHenry CL, Li Y, Feng W, et al. MERTK arginine-844-cysteine in a patient with severe rod-cone dystrophy: loss of mutant protein function in transfected cells. *Invest Ophthalmol Vis Sci.* 2004;45: 1456–1462.
13. Tschernutter A, Jenkins SA, Waseem NH, et al. Clinical characterization of a family with retinal dystrophy caused by a mutation in the Mertk gene. *Br J Ophthalmol.* 2007;90:718–723.
14. Brea-Fernandez AJ, Pomares E, Brion MJ, et al. Novel splice donor site mutation in MERTK gene associated with retinitis pigmentosa. *Br J Ophthalmol.* 2008;92:1419–1423.
15. Bourne MC, Campbell DA, Tansley K. Hereditary degeneration of the rat retina. *Br J Ophthalmol.* 1938;22:613–623.
16. Dowling JC, Sidman RL. Inherited retinal dystrophy in the rat. *J Cell Biol.* 1962;14:73–109.
17. Mullen RJ, LaVail MM. Inherited retinal dystrophy: primary defect in pigment epithelium determined with experimental rat chimeras. *Science.* 1976;192:799–801.
18. D'Cruz PM, Yasumura D, Weir J, et al. Mutation of the receptor tyrosine kinase gene Mertk in the retinal dystrophic RCS rat. *Hum Mol Genet.* 2000;4:645–651.
19. Vollrath D, Feng W, Duncan JL, et al. Correction of the retinal dystrophy phenotype of the RCS rat by viral gene transfer of Mertk. *Proc Natl Acad Sci U S A.* 2001;26:12584–12589.
20. Camenisch TD, Koller BH, Earp HS, Matsushima GK. A novel receptor tyrosine kinase, Mer, inhibits TNF-a production and lipopolysaccharide-induced endotoxic shock. *J Immunol.* 1999; 162:3498–3503.
21. Duncan JL, LaVail MM, Yasumura D, et al. An RCS-like retinal dystrophy phenotype in Mer knockout mice. *Invest Ophthalmol Vis Sci.* 2003;44:826–838.
22. Feng W, Yasumura D, Matthes MT, LaVail MM, Vollrath D. Mertk triggers uptake of photoreceptor outer segments during phagocytosis by cultured retinal pigment epithelial cells. *J Biol Chem.* 2002;19:17016–17022.
23. Hall MO, Obin MS, Heeb MJ, Burgess BL, Abrams TA. Both protein s and gas6 stimulate outer segment phagocytosis by cultured rat retinal pigment epithelial cells. *Exp Eye Res.* 2005; 81:581–591.
24. Collin GB, Cyr E, Bronson R, et al. Alms1-disrupted mice recapitulate human Alstrom syndrome. *Hum Mol Genet.* 2005;14:2323–2333.
25. Scott RS, McMahon EJ, Pops SM, et al. Phagocytosis and clearance of apoptotic cells is mediated by Mer. *Nature.* 2001;411:207–211.
26. Dick AD, Forrester JV, Liversidge J, Cope AP. The role of tumour necrosis factor (TNF-alpha) in experimental autoimmune uveoretinitis (EAU). *Prog Retin Eye Res.* 2004;23:617–637.
27. Theodossiadis PG, Liarakos VS, Sfikakis PP, Vergados IA, Theodossiadis GP. Intravitreal administration of the anti-tumor necrosis factor agent infliximab for neovascular age-related macular degeneration. *Am J Ophthalmol.* 2009;147:825–830, 830.e1.
28. Saxena S, Pant AB, Khanna VK, et al. Interleukin-1 and tumor necrosis factor-alpha: novel targets for immunotherapy in Eales disease. *Ocul Immunol Inflamm.* 2009;17:201–206.
29. Salama B, Gicquel JJ, Lenoble P, Dighiero PL. Optic neuropathy in refractory neurosarcoidosis treated with TNF-alpha antagonist. *Can J Ophthalmol.* 2006;41:766–768.
30. Theodossiadis PG, Markomichelakis NN, Sfikakis PP. Tumor necrosis factor antagonists: preliminary evidence for an emerging ap-

proach in the treatment of ocular inflammation. *Retina.* 2007;27: 399–413.

31. Adán A, Sanmarti R, Burés A, Casaroli-Marano RP. Successful treatment with infliximab in patients with diffus subretinal fibrosis syndrome. *Am J Ophthalmol.* 2007;143: 533–534.
32. Nakazawa T, Nakazawa C, Matsubara A, et al. Tumor necrosis factor-alpha mediates oligodendrocyte death and delayed retinal ganglion cell loss in a mouse model of glaucoma. *J Neurosci.* 2006;26:12633–12641.
33. LaVail MM, Unoki K, Yasumura D, Matthes MT, Yancopoulos GD, Steinberg RH. Multiple growth factors, cytokines and neurotrophins rescue photoreceptors from the damaging effects of constant light. *Proc Natl Acad Sci U S A.* 1992;89: 11249–11253.
34. Thanos S. Sick photoreceptors attract activated microglia from the ganglion cell layer: a model to study the inflammatory cascades in rats with inherited retinal dystrophy. *Brain Res.* 1992;588:21–28.